

Aero-Structural Optimization of the NASA Common Research Model

Stefan Keye* Thomas Klimmek† Mohammad Abu-Zurayk‡
Matthias Schulze§ Časlav Ilić¶
German Aerospace Center (DLR)

A combined aerodynamic and structural, gradient-based optimization has been performed on the NASA/Boeing Common Research Model civil transport aircraft configuration. The computation of aerodynamic performance parameters includes a Reynolds-averaged Navier-Stokes CFD solver, coupling to a linear static structural analysis using the finite element method to take into account aero-elastic effects. Aerodynamic performance gradients are computed using the adjoint approach. Within each optimization iteration, the wing's structure is sized via a gradient-based algorithm and an updated structure model is forwarded for the performance analysis. In this pilot study wing profile shape is optimized in order to study engine installation effects. This setting was able to improve the aerodynamic performance by 4%

I. Introduction

THE aircraft industry is continuously in the search for advanced designs that consume less fuel and produce less emissions. The *Flightpath 2050*^a provides a vision for Europe's aviation systems and industries by the year 2050. Concerning the environmental aspects, the vision expects a high reduction in CO₂ and NO_x emission per passenger kilometer, in addition to a 65% reduction in noise emission of air vehicles -by 2050- relative to those of the year 2000. On the other hand, the worldwide air traffic is predicted to grow by 4-5% per year, which makes the fulfillment of these expectations a highly challenging task.

Aircraft optimization, which can be performed using numerical techniques, is an indispensable choice to face the *Flightpath 2050* challenges and to increase the aircraft's efficiency. An optimization that incorporates more than one discipline is called a multidisciplinary design optimization (MDO). Employing MDO in aircraft design, yields realistic designs that fulfill the constraints of the engaged disciplines and reduces the development risks. Moreover, MDO reduces the design cycle of an aircraft. However, the complexity of the problem in MDO significantly increases when compared to single-disciplinary optimizations. Therefore, optimization algorithms that drive high-fidelity MDO need to be particularly efficient.

There are mainly two types of optimization algorithms, depending on whether the gradients information is required throughout the optimization; gradient-free algorithms and gradient-based algorithms. In the former, only the objectives and constraints values are required by the end of a design (or optimization) iteration. In the latter, on the other hand, the values and the gradients of the objectives and the constraints are required throughout the search for the optimum. The extra expense of these algorithms pays off as efficiency; gradient-based algorithms can reach an optimum more efficiently than gradient-free algorithms, at least the nearest (potentially local) optimum.

These characteristics of gradient-based algorithms make them good candidates for optimization problems that start from a good design and require some fine tuning. In this paper the wing of the Common Research

*Scientist, Dept. Transport Aircraft, Institute of Aerodynamics and Flow Technology, Lilienthalplatz 7, 38108 Braunschweig, Member AIAA.

†Scientist, Dept. Loads Analysis and Aeroelastic Design, Institute of Aeroelasticity, Bunsenstrasse 10, 37073 Göttingen.

‡Scientist, Center for Computer Applications in Aerospace Science and Engineering (C²A²S²E), Institute of Aerodynamics and Flow Technology, Lilienthalplatz 7, 38108 Braunschweig.

§Scientist, Dept. Loads Analysis and Aeroelastic Design, Institute of Aeroelasticity, Bunsenstrasse 10, 37073 Göttingen.

¶Scientist, Dept. Transport Aircraft, Institute of Aerodynamics and Flow Technology, Lilienthalplatz 7, 38108 Braunschweig.

^a<http://ec.europa.eu/transport/air/doc/flightpath2050.pdf>

Model (CRM)^b, which was designed without the propulsion system in place, is used as a starting point and optimized with the attached pylon and engine nacelle employing a gradient-based algorithm on local design parameters.

For a gradient-based optimization to be efficient, the evaluation of the gradient itself has to be efficient. There are several approaches for computing the gradients, of which the adjoint approach is the most efficient when the number of design variables in the problem is higher than the number of objectives and constraints. If otherwise, the finite difference approach is more efficient. The use of adjoint approach in MDO was pioneered by Martins¹ and followed by others^{2,3} for higher levels of fidelity.

Another basic element in MDO is the formulation (or architecture) that a MDO follows. It defines how the different disciplines are coupled and at what points during the optimization, it also describes which design variables are touched by which discipline or optimizer. Choosing the formulation depends on the nature and number of design variables, the nature and number of disciplines engaged and the type of optimization algorithms employed. Some studies were performed to identify the advantages of different architectures⁴ but there was only little testing of MDO architectures on real aircraft.⁵

The most visited MDO case in research is the aero-structural problem, since it includes two main disciplines in the aircraft design that directly affect the fuel consumption during a mission. In academics this problem was tackled intensively by Martins and his MDO group¹ where they showed several high-fidelity aero-structural optimizations with gradient-based algorithms on the CRM model among other configurations. In research organizations this problem was investigated by Ronzheimer² and Ilić⁶ where it was applied to a DO728 and the Airbus research aircraft configuration XRF-1, respectively, using gradient-free algorithms. Moreover, at ONERA,⁷ MDO was applied on the XRF-1 configuration using a bi-level optimization technique. Piperni et al.,⁸ on the other hand, showed a first complex application on aero-structural optimization by industry where it was applied on regional and business jets. The levels of fidelity here were compromised in some aspects though.

The aim of this paper is to perform a gradient-based, aero-structural optimization of the CRM wing while having the full configuration, with engine and tail. The aero-structural optimization problem consists mainly of two parts, the performance part which tries to find the optimum performance of the configuration, and the sizing part which guarantees that the wing will withstand the critical loads.

II. Optimization Problem Definition

At DLR two main optimization directions are currently investigated for developing novel and reusable MDO processes. The first direction gathers three levels of fidelity, starting from preliminary design, passing by a dynamic level for the prediction of critical load cases, and ending with a detailed high-fidelity aero-structural level. Due to the high complexity of this direction, it was decided here to engage a limited number of global design parameters that control the planform of the wing in addition to some main twist sections. The second direction concentrates on sharpening and exploring the gradient-based approach for high-fidelity MDO. Whilst the first direction aims at finding a global optimum for the design parameters and taking constraints from all levels of aircraft design, the second direction focuses at refining the optimum design produced by the global optimization and uses hundreds of local wing parameters on the aerodynamic and the structural sides to optimize the resulting aircraft using a gradient-based approach. This paper describes the studies performed in the second direction that adopts the high-fidelity gradient-based MDO.

The model employed in this study is the NASA Common Research Model civil transport aircraft configuration, Figure 1, designed by NASA's Subsonic Fixed Wing Technical Working Group and by Vassberg et al.⁹ Parameterization of the CRM is based on free-form deformation (FFD) for the wing shape, Figure 2, and variable shell element thicknesses for the wing structure, Figure 3. In this case, a FFD box is used to parameterize wing outer shape. On the structural side, the individual shell elements are clustered into different design fields and one thickness parameter is assigned to each field. Progression of the performance optimization is evaluated using DLR's fluid-structure interaction (FSI) simulation procedure¹⁰ to take into account aero-elastic effects. The FSI simulation couples DLR's Reynolds-averaged Navier-Stokes (RANS) flow solver TAU¹¹ and the commercially available finite element structural analysis code NASTRAN^{®c}.

The objective of the performance part of the optimization is the improvement of the lift to drag ratio and the objective of the sizing sub-problem is the reduction of mass under the design load cases.

^b<http://commonresearchmodel.larc.nasa.gov/>

^c<https://www.mssoftware.com/product/msc-nastran/>

A single-point optimization at a point close to the cruise design point ($Ma = 0.85$, $C_L = 0.535$) will be performed. The number of design parameters is 420 for the aerodynamic shape and 322 for the structural thicknesses. The structural model is pre-sized with a set of 16 load cases from low-fidelity methods. In common gradient-based optimizations, since the global design parameters like planform or sweep angle are fixed and changes in wing shape remain small, it is assumed that the critical load cases do not change and therefore no sizing loops are performed during the optimization. Alternatively, when it turns out that the number of critical load cases does vary, which is possible because they are computed for each design by the structural model generator using low-fidelity methods, the bi-level integrated system synthesis (BLISS)^{7,12} can be used. In this study, a selected number of load cases is used within each design iteration to size the wing as will be shown in details.

III. Gradient-Based Aero-Structural Optimization Architecture

The MDO architecture employed here is shown in Figure 4. The optimizer uses the Sequential Quadratic Programming (SQP) algorithm from the optimization framework Pyranha (Python based framework for optimizations relying on high-fidelity approach).¹³

The optimizer suggests the outer shape design variables, and the CFD and the computational structural mechanics (CSM) models are updated accordingly. On the CFD side, the update is applied directly onto the grid using mesh deformation, whereas on the CSM side, a new structural model is built into the updated geometry. This is done by applying the so-called MONA process. The MONA process, described in Section IV.B below, is a loads analysis and structural optimization process based on a parametric set-up of all involved simulation and optimization models. When the sizing process is completed, the sized CSM model is forwarded to the performance side in order to compute the flow-structure states. Then the states are forwarded to the gradient-computation tools on the performance side, where the aerodynamic gradients are computed for the aero-elastically coupled wing. Finally, the gradients together with the performance state are forwarded to the optimizer in order to update the shape design variables.

Since obtaining the interdisciplinary or cross gradients, i.e. derivatives of aerodynamic parameters w.r.t. structural design variables and vice versa, is very expensive, and since these gradients have less effect on the optimization than the disciplinary gradients as noticed in previous tests,¹⁴ the interdisciplinary gradients are neglected here.

IV. Numerical Models

IV.A. CFD Grid

An unstructured, hybrid, hex-dominated, CFD grid was generated on the CRM geometry using the commercial grid generation package SOLAR.¹⁵ The grid was built according to the gridding guidelines of the 6th AIAA Computational Fluid Dynamics Drag Prediction Workshop (DPW-6)^d. To make the grid suitable for optimization overall grid size has been considerably reduced to approximately 7.0 million points and 43 boundary layers on all viscous walls. Preliminary CFD test runs showed good convergence and an accurate prediction of aerodynamic parameters. The capability to compute aerodynamic performance gradients utilizing the adjoint approach has also been tested successfully.

IV.B. Finite Element Model and further Simulation Models of the MONA Process

The CRM structural model is built using a NASTRAN[®]-based CSM model generator ModGen¹⁶ developed by DLR's Institute of Aeroelasticity. The updated structural model is the result of the MONA process. The name MONA represents the main computer programs involved in the sub-process, ModGen and MSC Nastran.

The first step of MONA is the set-up of parameterized simulation models with ModGen, including an initial finite element model, an aerodynamic model for the doublet lattice method (DLM), mass models, and an optimization model for the structural variables and constraints, are set up, based on the outer geometry and a given structural design concept. This approach enables a wide range of parameter variations, combined with a sound structural design.

^dhttp://aiaa-dpw.larc.nasa.gov/Workshop6/DPW6_gridding_guidelines_2015-08-28.pdf

The second step performs a loads analysis for selected mass configurations and flight conditions using the flexible aircraft structure. MSC Nastran is taken for the loads analysis using the structural model of the complete aircraft. As MSC Nastran aeroelastic loads analysis uses the DLM for the aerodynamic part of the loads, it offers on the one hand the opportunity to estimate a high number of load cases for maneuver and gust conditions and on the other hand the prospect to include also CFD results in terms of correction factors and matrices for the actually subsonic but fast DLM. As the presented paper is the first application of MONA within the established MDO architecture only four load cases are taken into account.

In the third step the structure of the wing box is sized using gradient based structural optimization methods of MSC Nastran. Additionally, the sensitivities of the structural variables with respect to the structural constraints are computed. Though the sensitivity analysis is done with finite differences or semi-analytically, it is deeply nested in the structural analysis and related to the set-up of the system matrices for structural analysis. Therefore the structural sensitivity analysis is also very efficient. The structural design variables are the shell element thickness values. Groups of elements, e.g. the skin between two adjacent ribs and spars, are clustered into design fields. The structural constraints in the presented paper are the allowable stress values for each finite element and local buckling safety factors. Furthermore aileron effectiveness can be defined as structural constraints in order to avoid control surface reversal.

V. Results

The goal of the first aero-structural optimization test case was to investigate modifications of the aerodynamic wing shape and flow features, caused in part by fitting an engine nacelle and pylon to the CRM baseline wing, which was designed without a propulsion system. It is therefore assumed that wing shape modifications introduced by the optimizer around the nacelle location are in some way related to engine installation effects. Parameterization includes 420 FFD control points for the wing's outer shape and 322 wing box shell thicknesses for the inner wing structure. A single-point optimization has been performed at a point close to the cruise design point ($Ma = 0.85$, $h = 35000\text{ft}/10668\text{m}$, $C_L = 0.535$).

In Figure 5 the lift to drag ratio is plotted over the number of optimization loops. Only those data points where drag is improved over the baseline value are shown. Total drag is reduced from 285.8dc to 274.9dc within 16 design iterations. Most of that reduction already occurs over the first optimization cycle.

Figure 6 shows the chordwise static pressure distribution and profile section geometry for six spanwise coordinates. Sections no. 3 ($\eta = 0.300$) and no. 4 ($\eta = 0.375$) are located aside the nacelle on the inboard and outboard side, respectively. Figure 7 shows the surface pressure distributions for both the baseline and the optimized configuration.

Profile shape variations were found to be generally small, as it is expected for a gradient-based optimization. The largest surface deflections occur on the wing upper side. Their location appears to be associated with shock location and their magnitude relates to shock strength. Shape variations of the profile sections adjacent to the engine nacelle are not significantly larger than for the other wing sections. Apparently, drag reduction is mostly driven by transonic effects, i.e. the reduction of shock strength. Overall, the observed tendency to reduce shock strength and the corresponding wave drag and eliminate the double-shock pattern on the outboard wing corresponds to results found with other single-point optimization studies. Additionally, as shown in Figure 8, the lift distribution along the span tends to become more elliptic during the optimization and hence reducing the induced drag.

For the various optimization loops the resulting mass of the load carrying wing box differs within the margin of +4.3% and -1.6%. The baseline wing box has a mass of 10277 kg and the value for optimization step 16 is 10483 kg (2% increase). The small margin shows that the nominal changes of the aerodynamic shape have an insignificant influence on the structural weight of the wing. This is supported by the results of the loads analysis, where the root bending moment is increased by 1.3% from baseline to optimization step 16.

The thickness distribution of the optimized CRM-baseline wing box is shown in Figure 9. The distribution is reasonable compared to previous results¹⁶. As expected, the highest thickness values are located at the kink, where the high values of stress usually occur. At the wingtip the thickness of the skin goes down to minimum thickness of 2 mm due to manufacturing constraints. As the resulting wing box mass values, differences of the thickness distribution are also more or less marginal.

Conclusions

A combined aerodynamic and structural, gradient-based optimization has been performed on the Common Research Model civil transport aircraft configuration. The aerodynamic shape parameterization uses a free-form deformation approach, structural parameterization includes variable shell thicknesses of the wing box. A single-point optimization close to the cruise design point has been performed. The loads analysis and the structural optimization of the wing box show only marginal effects on the structural mass of the wing box. The next steps would investigate the engine integration effects on the aero-structure optimization.

Acknowledgments

The research presented in this paper has been performed in part in the framework of the European research project AGILE (Aircraft 3rd Generation MDO for Innovative Collaboration of Heterogeneous Teams of Experts) and has received funding from the European Union Horizon 2020 Program (H2020-MG-2014-2015) under grant agreement no 636202.

References

- ¹Kenway, G., Kennedy, G., and Martins, J., “A Scalable Parallel Approach for High-Fidelity Aerostructural Analysis and Optimization,” AIAA Paper 2012–1922, April 2012.
- ²Brezillon, J., Abu-Zurayk, M., Ronzheimer, A., Haar, D., Krüger, W., and Lummer, M., “Development and application of multi-disciplinary optimization capabilities based on high-fidelity methods,” AIAA Paper 2012–1757, April 2012.
- ³Ghazlane, I., Carrier, G., Dumont, A., and Désidéri, J.-A., “Aerostructural Adjoint Method for Flexible Wing Optimization,” AIAA Paper 2012–1924, April 2012.
- ⁴Martins, J. and Lambe, A., “Multidisciplinary Design Optimization: A Survey of Architectures,” *AIAA Journal*, Vol. 51, No. 9, pp. 2049–2075, 2013.
- ⁵Defoort, S. et al., “Multidisciplinary Aerospace System Design: Principles, Issues and Onera Experience,” *Aerospace Lab Journal*, Issue 4, 2012.
- ⁶Ilić, C. et al., “Comparison of Breguet and ODE Evaluation of the Cruise Mission Segment in the Context of High-Fidelity Aircraft MDO,” Vol. 132, 2016, pp. 87–97, 19th STAB/DGLR Symposium 2014.
- ⁷Blondeau, C., Irisarri, F., Leroy, F., and Salah El Din, I., “A Bi level high fidelity Aero structural integrated design Methodology,” 3rd Aircraft Structural Design Conference, RaeS, October 2012.
- ⁸Piperni, P., Abdo, M., and Kafyeke, F., “The Application of Multi-Disciplinary Optimization Technologies to the Design of a Business Jet,” AIAA Paper 2004–4370, 2004.
- ⁹Vassberg, J., DeHaan, M., Rivers, S., and Wahls, R., “Development of a Common Research Model for Applied CFD Validation Studies,” Paper 2008–6919, AIAA, June 2008.
- ¹⁰Heinrich, R., Wild, J., Streit, T., and Nagel, B., “Steady Fluid-Structure Coupling for Transport Aircraft,” ONERA-DLR Aerospace Symposium, Oct. 2006.
- ¹¹Gerhold, T., “Overview of the Hybrid RANS Code TAU,” *MEGAFLOW*, edited by N. Kroll and J. Fassbender, Vol. 89 of *Notes on Numerical Fluid Mechanics and Multidisciplinary Design*, Springer, 2005, pp. 81–92.
- ¹²Sobieszczanski-Sobieski, J., Agte, J., and Jr., R. S., “Bilevel Integrated System Synthesis,” *AIAA Journal*, Vol. 38, No. 1, pp. 164–176, 2000.
- ¹³Brezillon, J. and Abu-Zurayk, M., “Aerodynamic Inverse Design Framework using Discrete Adjoint Method,” Vol. 121, 2013, pp. 489–496, 17th STAB/DGLR Symposium 2010.
- ¹⁴Abu-Zurayk, M., Ilic, C., Schuster, A., and Liepelt, R., “Effect of Gradient Approximations on Aero-Structural Gradient-based Wing Optimization,” EUROGEN 2017, Abstract submitted, 2017.
- ¹⁵Martineau, D., Stokes, S., Munday, S., Jackson, A., Gribben, B., and Verhoeven, N., “Anisotropic Hybrid Mesh Generation for Industrial RANS Applications,” AIAA Paper 2006-0534, Jan. 2006.
- ¹⁶Klimmek, T., “Parametric Set-Up of a Structural Model for FERMAT Configuration for Aeroelastic and Loads Analysis,” *Journal of Aeroelasticity and Structural Dynamics*, Vol. 3, No. 2, pp. 31–49, 2014.

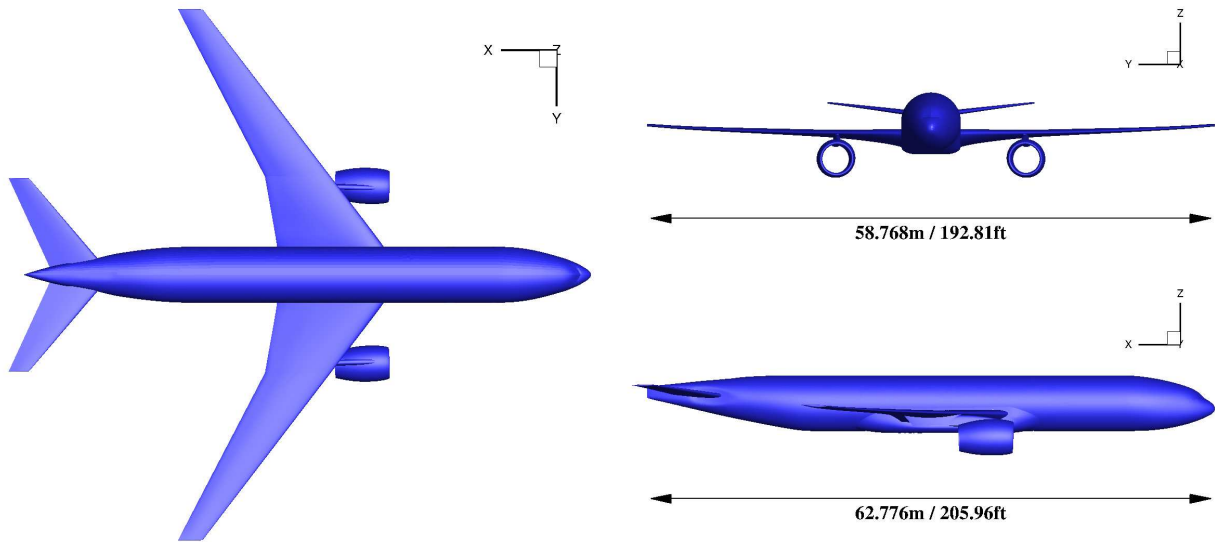


Figure 1. NASA Common Research Model, configuration including wing, body, nacelles, and pylons.

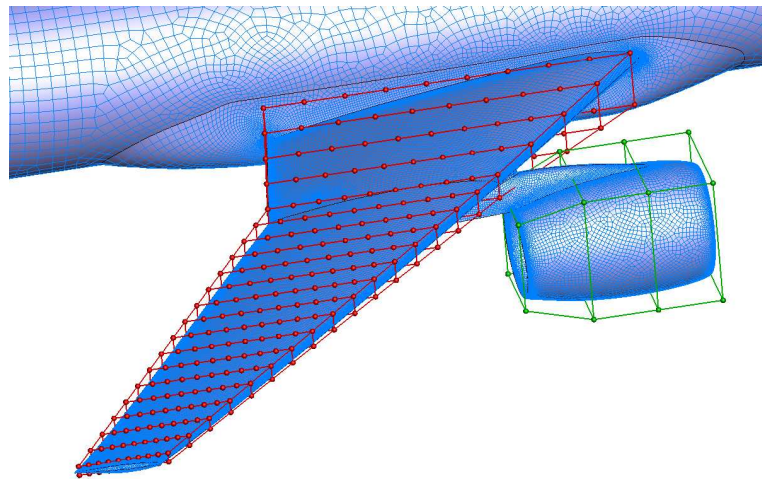


Figure 2. CFD surface grid and FFD boxes for aerodynamic shape parameterization.

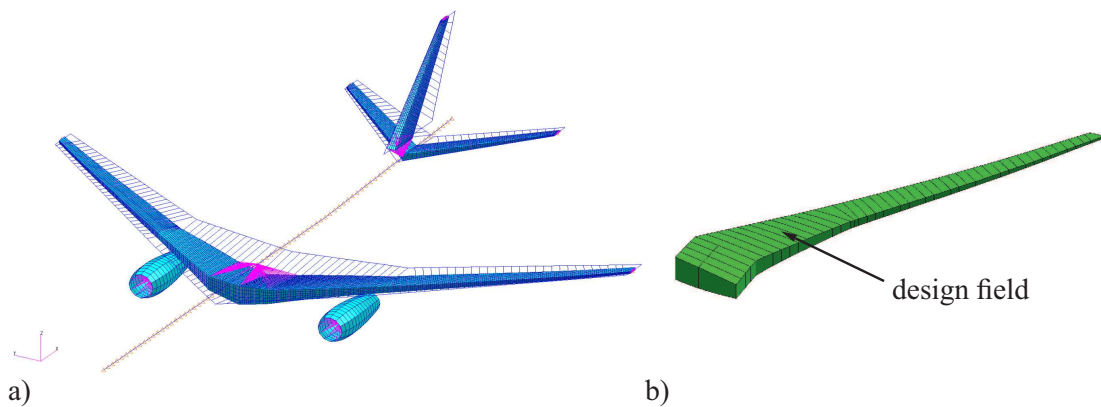


Figure 3. Structural model of wing box, a) shell elements, b) design fields for element clustering.

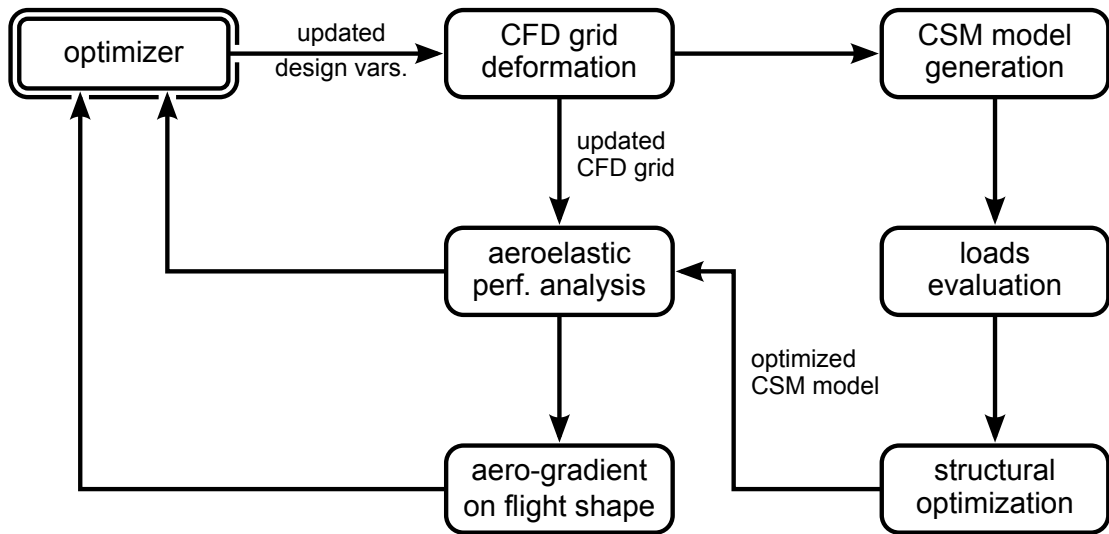


Figure 4. High-fidelity gradient-based MDO.

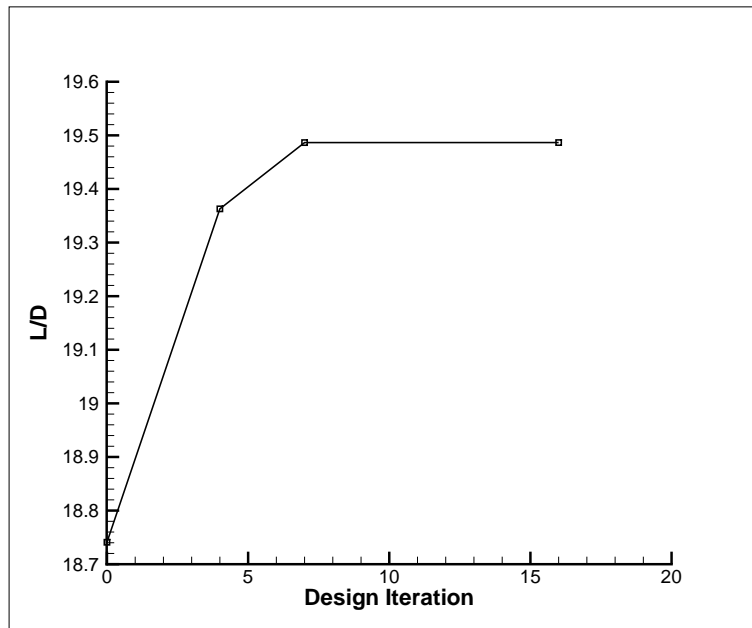


Figure 5. Convergence of total drag coefficient with optimization loop number.

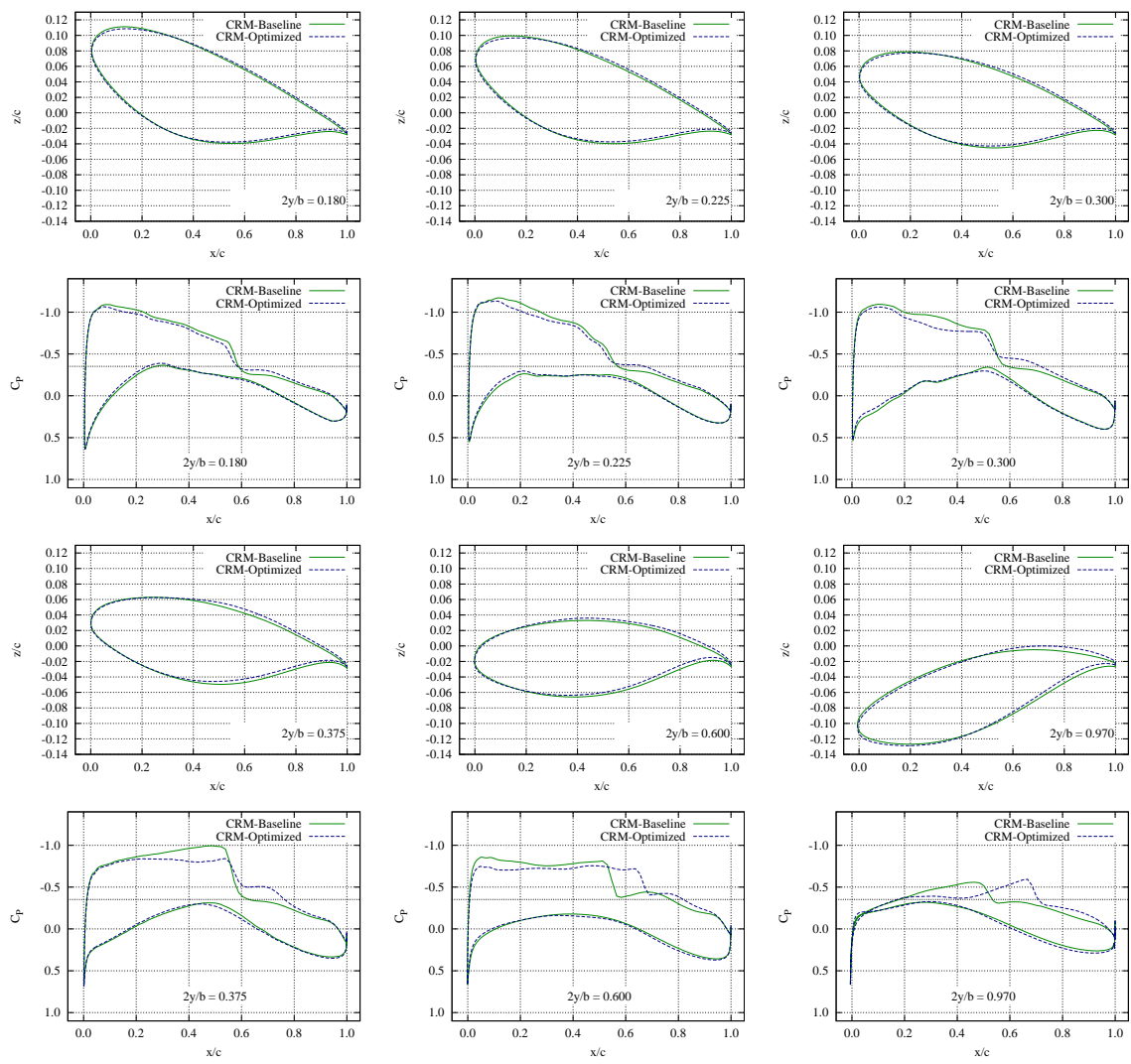


Figure 6. Comparison of wing profile section geometries and static pressure distributions for baseline and optimized wing.

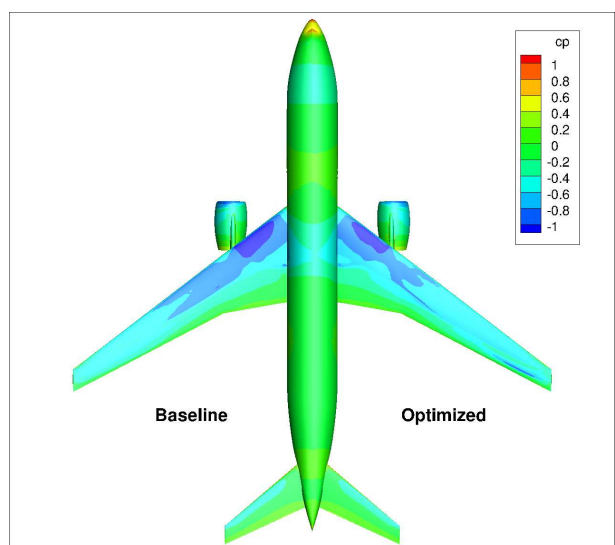


Figure 7. Comparison of pressure distribution for baseline and optimized configurations

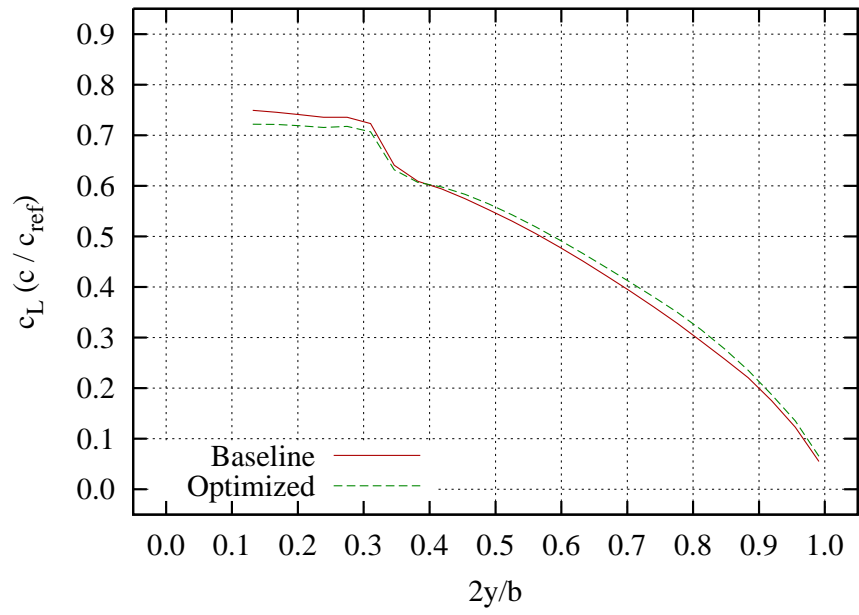


Figure 8. Comparison of spanwise lift distribution for baseline and optimized configuration

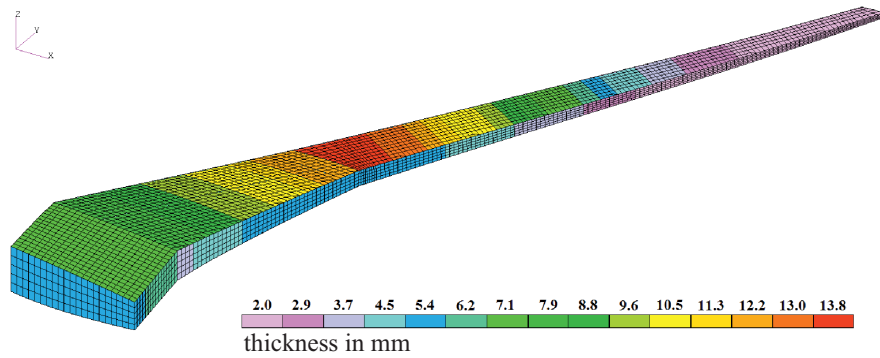


Figure 9. Thickness distribution of the optimized sized wing box of the baseline configuration